A&A 447, 1153–1158 (2006)
DOI: 10.1051/0004-6361:20053742

Astronomy & Astrophysics

The size and albedo of Rosetta fly-by target 21 Lutetia from new IRTF measurements and thermal modeling

M. Mueller[1], A. W. Harris[1], S. J. Bus[2], J. L. Hora[3], M. Kassis[4], and J. D. Adams[5]

[1] DLR Institute of Planetary Research, Rutherfordstr. 2, 12489 Berlin, Germany
e-mail: michael.mueller@dlr.de
[2] Institute for Astronomy, 640 North A'ohoku Place, Hilo, HI 96720, USA
[3] Harvard-Smithsonian Center for Astrophysics, 60 Garden Street, MS-65, Cambridge, MA 02138-1516, USA
[4] Keck Observatory, 65-1120 Mamalahoa Highway, Kamuela, HI 96743, USA
[5] Cornell University, 206 Space Science Bldg., Ithaca, NY 14853, USA

Received 1 July 2005 / Accepted 11 October 2005

ABSTRACT

Recent spectroscopic observations indicate that the M-type asteroid 21 Lutetia has a primitive, carbonaceous-chondrite-like (C-type) surface composition for which a low geometric albedo would be expected; this is incompatible with the IRAS albedo of 0.221 ± 0.020. From new thermal-infrared spectrophotometric measurements and detailed thermophysical modeling we infer that Lutetia has a diameter of 98.3 ± 5.9 km and a geometric albedo of 0.208 ± 0.025, in excellent agreement with the IRAS value. We can thus rule out a low albedo typical of a C-type taxonomic classification. Furthermore, we find that Lutetia's thermal properties are well within the range expected for large asteroids; we find no evidence for unusually high thermal inertia.

Key words. minor planets, asteroids – infrared: solar system – radiation mechanisms: thermal

1. Introduction

During its journey to the comet 67P/Tschurjumow-Gerasimenko, the ESA spacecraft Rosetta is scheduled to fly by two main-belt asteroids (Barucci et al. 2005): 2867 Šteins in September 2008 and 21 Lutetia in July 2010. Due to its small size of just a few kilometers, little is known about Šteins. On the other hand, Lutetia with a diameter of about 100 km is rather well observed at various wavelengths. However, the emerging picture of its surface composition is ambiguous: based on color measurements and the IRAS albedo of 0.221 ± 0.020, Tholen (1989) classified Lutetia as M-type, therefore it was generally believed to have a metallic surface composition. Howell et al. (1994) confirm this classification using a larger data set (they noted that Lutetia has an affinity to the C-class but ruled it out on the basis of the IRAS albedo). Based on CCD spectroscopy, Bus & Binzel (2002) classified Lutetia as X_k-type, which is compatible with a metallic surface composition. However, in recent work by Birlan et al. (2004), Lazzarin et al. (2004), and Barucci et al. (2005), spectral features were found, which are similar to those of carbonaceous chondrites. This seems to hint at a more "primitive" surface composition, which is usually associated with a C-type classification and a geometric albedo below 0.1, incompatible with the IRAS value. Interestingly, Lupishko & Mohamed (1996) derived a geometric albedo of 0.100 from polarimetry. Also, Magri et al. (1999) found Lutetia's radar albedo to be the lowest measured for any M-type main-belt asteroid – metallic objects are expected to display a *high* radar albedo. Furthermore, results of Rivkin et al. (2000) and Lazzarin et al. (2004) indicate the presence of hydrated material on Lutetia's surface.

In short, the IRAS albedo seems incompatible with recent results. Barucci et al. (2005) thus called for a new determination of Lutetia's albedo.

The observed thermal emission of an asteroid is determined by its shape, size, albedo, thermal inertia, surface roughness, and spin-state. The derivation of radiometric diameters and albedos requires an appropriate thermal model to describe the temperature distribution on the asteroid and the observing geometry. Radiometric results can be flawed if an over-simplified model is used.

We employed two independent thermal models with different levels of sophistication, both of which should be more reliable than the simple "standard thermal model" used by Tedesco (1992) in the derivation of IRAS albedos. The radiometric diameters and albedos resulting from the thermal models are in excellent agreement. Furthermore, both models indicate that Lutetia's thermal properties are well within the range expected for large main-belt asteroids.

Table 1. Observing geometry and modeling assumptions (H and G are from Tedesco 1992).

Heliocentric distance r	2.065 AU
Geocentric distance Δ	2.199 AU
Solar phase angle α	27.4°
Absolute magnitude H	7.35
Slope parameter G	0.11
Thermal emissivity ϵ	0.9

Table 2. Observations of 21 Lutetia. Times are those of mid exposure on June 24, 2004 and are not light-time corrected. Filter "V" denotes an Apogee measurement; numbers denote the central wavelength (in μm) of the MIRSI filter used.

UT	Filter	Flux	$\sigma_{\rm Flux}$
14:17	V	11.87 mag	0.01 mag
14:19	11.6	12.88 Jy	1.29 Jy
14:26	8.7	5.81 Jy	0.58 Jy
14:34	18.4	17.1 Jy	4.1 Jy
14:37	V	11.81 mag	0.01 mag

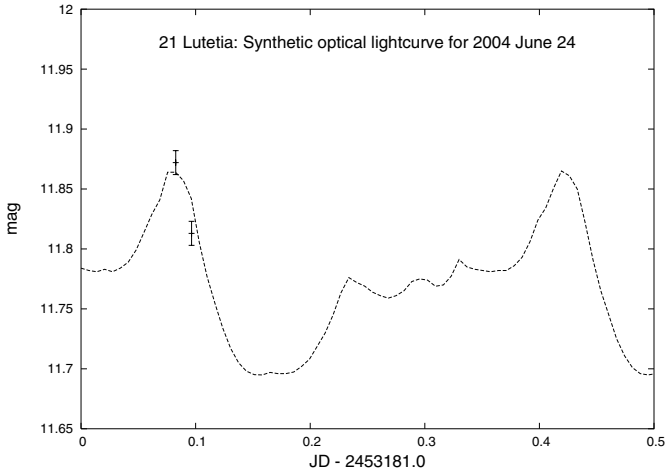

Fig. 1. Measured V-band data (see Table 2) and synthetic optical lightcurve generated using the shape model by Torppa et al. (2003). The rotational period is 8.165455 h, so some 1.5 cycles are displayed.

2. Observations

The observations were performed on June 24, 2004, between roughly 14:15 and 15:00 UT, at the NASA infrared telescope facility (IRTF) on Mauna Kea using the mid-infrared spectrometer and imager MIRSI (Deutsch et al. 2003) in imaging mode. Observing conditions were good with low humidity and no discernable clouds. See Table 1 for the observing geometry.

We observed Lutetia with MIRSI using three narrow-bandwidth filters centered at 8.7, 11.6, and 18.4 μm. The photometry was calibrated against subsequent observations of the standard stars γ Aql and β Peg, for which absolutely calibrated spectra have been published by Cohen et al. (1996, 1999). We also obtained absolutely calibrated V-magnitudes of Lutetia just before and just after the MIRSI observations, using Apogee, an optical CCD-camera installed at the IRTF. These were calibrated against the Landolt (1973) standard star 93-101.

We used a combination of Eric Volquardsen's data reduction pipelines for MIRSI and Apogee provided by the IRTF (`http://irtfweb.ifa.hawaii.edu/elv`) and standard synthetic aperture photometry routines. See Table 2 for a list of the optical and thermal-IR fluxes. For MIRSI N-band data (8.7 and 11.6 μm), the errors are dominated by the calibration uncertainty including possible atmospheric variability between observations; this uncertainty was estimated to be 10%. For the Q-band filter centered at 18.4 μm, uncertainties caused by the airmass correction and the statistical scatter resulting from the synthetic aperture procedure contributed an additional 14% to the error budget.

3. Data analysis

3.1. Observing geometry and rotational phase

From the inversion of multi-epoch optical lightcurves observed from 1962 through 1998, Torppa et al. (2003) derived a physical model of Lutetia's shape and spin state. Two pole directions are given, one of which seems to be superior to the other one (M. Kaasalainen, private communication, 2005). The J2000 ecliptic latitude of both solutions is +3°, the longitude is 39° for the preferred first solution and 220° for the secondary. This implies that during our observations, on 2004 June 24, the sub-Earth and sub-solar latitudes were −75° and −48°, respectively. Using the second pole orientation results in the same sub-Earth and sub-solar latitudes, but with their signs changed.

The shape model of Torppa et al. (2003) was used to generate a synthetic optical lightcurve. In Fig. 1 the resulting lightcurve is plotted, together with our measured V-band data. Judging from Fig. 1 our observations took place near lightcurve minimum; the lightcurve amplitude is roughly 0.17 mag from minimum to maximum.

Between 1983 Apr 25 and May 4, Lutetia was sighted five times by IRAS (Tedesco 1992); the observing geometry was practically constant, with a sub-Earth latitude of about 18° and a sub-solar latitude of about −2°. Again, choosing the second pole solution changes the signs.

3.2. NEATM

3.2.1. Description of the model

Despite its name, the "near-Earth asteroid thermal model" NEATM (Harris 1998) is applicable to all atmosphere-less bodies. It is a modification of the "standard thermal model" STM (Lebofsky et al. 1986) used in the derivation of IRAS diameters and albedos (Tedesco 1992). In contrast to the STM, the NEATM does not *assume* a color temperature for the thermal continuum, but is rather used to *derive* the apparent color temperature from which information on the thermal properties can be extracted.

Both the STM and NEATM are based on spherical geometry. In both models, local temperatures are assumed to be in instantaneous equilibrium with the incident solar flux, so

$$T(\psi) = T_{\rm SS} \cos^{1/4} \psi \quad (1)$$

where ψ is the angular distance from the sub-solar point and $T_{\rm SS}$ is the sub-solar temperature. Both models incorporate a dimensionless parameter η, which affects the apparent color temperature in the following way:

$$\eta {T_{\rm SS}}^4 \propto \text{absorbed solar flux at the sub-solar point.} \quad (2)$$

A hypothetical smooth Lambertian surface without thermal inertia would have $\eta = 1$. Large main-belt asteroids tend to display a slightly lower η, which corresponds to a higher apparent color temperature. This is thought to be caused by thermal-infrared "beaming" due to surface roughness, which at low phase angles gives rise to an elevated apparent surface temperature. An η value larger than unity indicates the presence of a cooling effect, which is thought to be thermal conduction into the subsoil, giving rise to significant thermal inertia. In the STM, η has the fixed value of 0.756, whereas in the NEATM η is treated as a fitting parameter that forces the model color temperature to match the observed one and thus allows a first-order correction for the above-mentioned effects.

3.2.2. Results

We have fitted both our new MIRSI data as given in Table 2 and the IRAS flux values published by Tedesco (1992). IRAS was equipped with four broad-band filters centered at 12, 25, 60, and 100 μm. The filter breadth requires color corrections of the fluxes (Beichman et al. 1988; see also `http://irsa.ipac.caltech.edu/IRASdocs/exp.sup/ch6/C3.html`) – we assumed a black-body temperature of 230 K. We considered only the 12, 25, and 60 μm filters since there are significant uncertainties concerning both the calibration of the 100 μm data and the applicability of the model at these wavelengths. All five IRAS sightings of Lutetia were used.

Throughout our data analysis we assumed Lutetia's thermal emissivity to be 0.9, and its absolute (optical) magnitude in the HG-system (Bowell et al. 1989) to be $H = 7.35$ with $G = 0.11$ (Tedesco 1992). In the HG-system, diameter and geometric albedo p_V are related by (see, e.g., Fowler & Chillemi 1992)

$$D = 10^{-H/5} \frac{1329 \text{ km}}{\sqrt{p_V}}. \quad (3)$$

See Table 3 for an overview of the NEATM results. The mean results from the IRAS data are $p_V = 0.197 \pm 0.027$, $D = 102.0 \pm 7.1$ km, and $\eta = 0.94 \pm 0.08$ (errors are from the internal scatter only), in excellent agreement with our MIRSI results.

Comparison of NEATM results with those derived by other techniques indicates that NEATM diameters and albedos are generally accurate to within 15% and 30%, respectively. Our final results with conservative uncertainties are given in Table 4.

Table 3. NEATM fits to the available thermal-infrared data: the MIRSI data as given in Table 2, and the five IRAS sightings (Tedesco 1992). No attempt at lightcurve-correction was made.

	η	p_V	D (km)
MIRSI	0.93	0.188	103.8
IRAS 1	0.93	0.178	106.6
IRAS 2	0.94	0.226	94.7
IRAS 3	1.06	0.161	112.2
IRAS 4	0.96	0.191	103.0
IRAS 5	0.82	0.231	93.6

Table 4. NEATM diameters and albedos of Lutetia for the two data sets.

	D (km)	p_V
MIRSI	104 ± 16	0.188 ± 0.057
IRAS (mean of five)	102 ± 16	0.197 ± 0.059

We did not attempt to correct our data to the flux level of the lightcurve average; if the shape model by Torppa et al. (2003) adequately describes the epoch of our observations (see Sect. 3.1), this should lead to a slight underestimation of the diameter of up to a few percent, well inside the range of uncertainty quoted.

Walker (2003) calculated a mean value for η of 1.067 ± 0.087 from IRAS observations of 694 asteroids. Our result for Lutetia, $\eta = 0.94 \pm 0.08$, is comparable to that of Walker (2003), which indicates that Lutetia has thermal properties rather typical for a large main-belt asteroid, i.e. low thermal inertia and some surface roughness.

3.3. Thermophysical model (TPM)

3.3.1. Description of the model

In this section we describe the analysis of our data using a detailed thermophysical model similar to that proposed by Lagerros (1996, 1998). The Lagerros model has found frequent application, primarily in the analysis of high-quality mid-infrared photometry and spectroscopy of large asteroids both for scientific purposes (see, e.g., Dotto et al. 2000) and to facilitate the use of asteroids as mid-infrared calibration standards (Müller & Lagerros 2002). Recently, it has also found application to thermal-infrared data of much smaller asteroids (cf. Müller et al. 2004; Harris et al. 2005; Mueller et al. 2005).

As the basis of our thermophysical modeling we use the shape model of Torppa et al. (2003) discussed in Sect. 3.1, which consists of a convex mesh of 2040 triangular facets. We model surface roughness by adding craters to each facet as sections of hemispheres. For the crater opening angle and the crater density, i.e. the percentage of the surface covered with craters, we have adopted the values from Müller et al. (2004) corresponding to "low", "default", and "high" roughness. The solar energy incident on a facet is calculated from the heliocentric distance and angle of inclination. Shadowing and multiple reflections of incident solar and thermally emitted radiation inside craters are fully taken into account using assumed

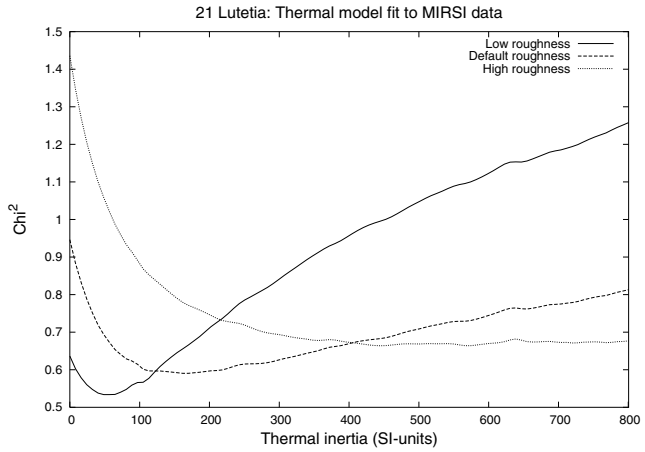

Fig. 2. Goodness of fit χ^2 vs. thermal inertia for the MIRSI data. For each value of thermal inertia, the best-fitting diameter is found. SI-units of thermal inertia are J m^{-2} s$^{-0.5}$ K^{-1}.

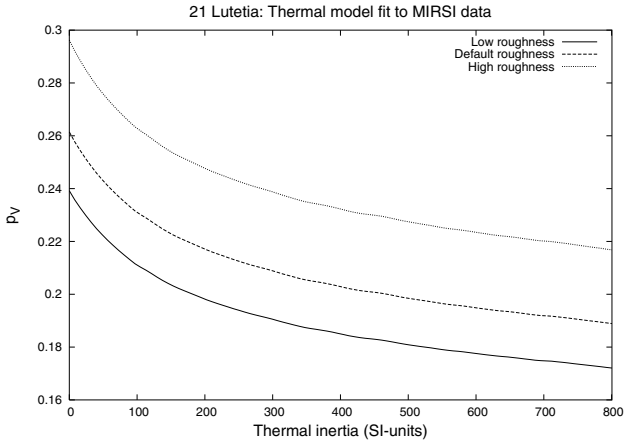

Fig. 3. Best-fit geometric albedo p_V vs. thermal inertia for the MIRSI data; cf. Fig. 2.

values of albedo and infrared emissivity. The temperature of each facet is determined by numerically solving the heat diffusion equation using an assumed value of thermal inertia. The total observable thermal emission is calculated by summing the contributions from all facets visible to the observer. Model parameters are adjusted until the best agreement with the observational data is obtained, i.e. χ^2 is minimized, thereby constraining the physical properties of the asteroid.

In contrast to simpler models such as the STM or the NEATM, the TPM can be consistently applied to multi-epoch data, see, e.g., Mueller et al. (2005), because it contains no empirical model parameters dependent on the observing geometry; rather it describes the asteroid purely in terms of intrinsic physical properties such as shape, size, and thermal inertia.

3.3.2. Results

It may not be appropriate to fit the MIRSI data with the TPM since its usage generally requires more than just three data points. As can be seen in Fig. 2, the best fit suggests low roughness and low thermal inertia of about 50 J m^{-2} s$^{-0.5}$ K^{-1}, which is comparable to the thermal inertia of lunar soil. However, considerably higher thermal inertias can also be fitted by adding more surface roughness (note the scale on the χ^2-axis!). According to Müller & Lagerros (1998), typical main-belt asteroid thermal inertias range between 5 and 25 J m^{-2} s$^{-0.5}$ K^{-1}.

Nevertheless, as can be seen in Fig. 3, the best-fit geometric albedo p_V for the respective best-fit thermal inertia is largely independent of surface roughness: $p_V = 0.225 \pm 0.020$ and $D = 94.9 \pm 4.3$ km, in excellent agreement with our NEATM-findings (Sect. 3.2.2). The uncertainties quoted here reflect only the scatter of the fitting procedure; we estimate the systematic uncertainties inherent in the modeling and calibration to be significantly higher: 10% for the diameter and 20% for albedo. Our MIRSI data alone do not significantly constrain Lutetia's thermal inertia or surface roughness.

We have also used the TPM to fit the flux values measured by IRAS in 1983 (see Sect. 3.2.2). As can be seen in Fig. 4, the IRAS data are also best fitted with a thermal inertia of about 50 J m^{-2} s$^{-0.5}$ K^{-1}. As in the case of the MIRSI data (see Fig. 2), the global minimum in χ^2 is situated at about the thermal inertia of lunar soil; however, this time the best fit is reached assuming high surface roughness as opposed to low surface roughness. The best-fit diameter and albedo are $p_V = 0.21 \pm 0.04$ and $D = 98.3 \pm 9.4$ km (statistical errors only – see above), in excellent agreement with our previous findings.

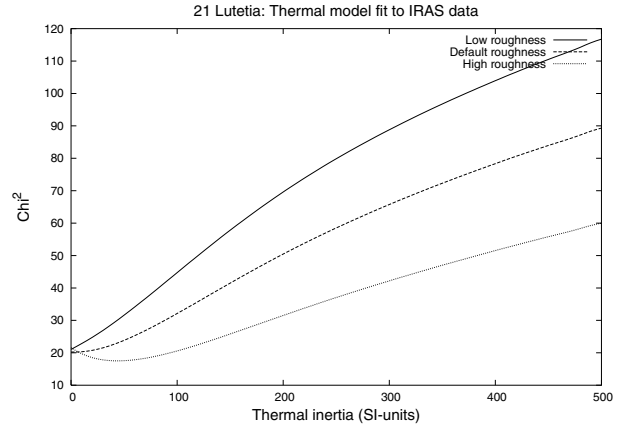

Fig. 4. As Fig. 2, but for IRAS data.

We have also attempted to simultaneously fit both data sets, MIRSI + IRAS. This leads to a best-fit thermal inertia of zero, whichever roughness is assumed. In particular, changing the roughness does not alter the goodness of the fit, so roughness is not constrained at all. The corresponding diameter and albedo are $p_V = 0.235 \pm 0.027$ and $D = 92.9 \pm 5.4$ km (statistical errors only), in agreement with our previous findings.

While the thermophysical model fits to the MIRSI, IRAS, and MIRSI + IRAS data sets give very similar values of D and p_V, results for thermal inertia and, in particular, surface roughness are not well constrained. However, our results strongly suggest that the thermal inertia does not greatly exceed 100 J m^{-2} s$^{-0.5}$ K^{-1}.

Table 5. Summary of diameter and albedo determinations for Lutetia. Values in parentheses are calculated by the authors on the basis of Eq. (3) and $H = 7.35$. NEATM results are quoted with 15 and 30% uncertainty in diameter and albedo, respectively; TPM results with 10% uncertainty in diameter and 20% uncertainty in albedo (see Sects. 3.2.2 and 3.3.2).

Source	Diameter (km)	p_V	Notes
Tedesco (1992)	95.8 ± 4.1	0.221 ± 0.020	Using the STM
Lupishko & Mohamed (1996)	(142.4)	0.100	From polarimetry
Magri et al. (1999)	116 ± 17	(0.151 ± 0.045)	From radar-observations
Present work	104 ± 16	0.188 ± 0.057	NEATM fit to MIRSI data
Present work	102 ± 16	0.197 ± 0.059	NEATM fit to IRAS data
Present work	94.9 ± 9.5	0.225 ± 0.045	TPM fit to MIRSI data
Present work	98.3 ± 9.9	0.210 ± 0.042	TPM fit to IRAS data
Present work	92.9 ± 9.3	0.235 ± 0.047	TPM fit to MIRSI+IRAS
Present work	98.3 ± 5.9	0.208 ± 0.025	Weighted average of rows 4—7

Linking multi-epoch data taken some 20 years apart requires very accurate knowledge of the rotational period. The one used in this work (8.165455 h) seems to be sufficiently accurate: it is based on a large temporal baseline of some 36 years (lightcurves from 1962–1998, including some from 1983), so it should safely bridge the six years 1998–2004. Judging from Fig. 1 this is indeed the case, although we caution that we have only two data points.

Another potential source of error is the sub-Earth latitude, which varies considerably between apparitions: in 1983, the sub-Earth latitude was +18°, as opposed to −75° in 2004 (see Sect. 3.1). This could cause the shape model to be biased towards one hemisphere, although we note that lightcurves at various sub-Earth latitudes were used in the construction of the shape model (for example, the sub-Earth latitude in Oct. 1962 was −54°). Furthermore, the surface composition or roughness could vary across the surface; our model assumes it to be homogeneous.

4. Discussion

4.1. Diameter and albedo

We have determined the radiometric size and albedo of 21 Lutetia from two data sets (IRAS and new IRTF measurements) and two independent thermal models with different levels of sophistication, see Sects. 3.2 and 3.3. Given the progress since the IRAS results in both thermal modeling (Harris 1998; Lagerros 1998) and mid-IR calibration (Cohen et al. 1996, 1999), our radiometric results should be more reliable than those of Tedesco (1992). Our results and those taken from the literature are summarized in Table 5. Given the uncertainties, there is good mutual agreement among the radar-results by Magri et al. (1999) and Tedesco's and our radiometric results, while the polarimetric albedo of Lupishko & Mohamed (1996) is inconsistent with all other albedo determinations. In particular, our results are incompatible with typical C-type albedos of ≤0.1, which may be indicated by recent spectroscopic findings (Birlan et al. 2004; Lazzarin et al. 2004; Barucci et al. 2005).

4.2. Thermal properties

From our data we have determined not only the radiometric diameter and albedo of Lutetia, but also the apparent color temperature, from which conclusions on the surface thermal properties, such as thermal inertia and roughness, can be drawn.

Using the NEATM, we found the fit parameter η, which describes the apparent color temperature, to be 0.93 / 0.94 for the MIRSI / IRAS-observations, respectively. This implies that Lutetia's thermal properties are rather typical for a main-belt asteroid, i.e. low thermal inertia and some surface roughness.

Our results from the thermophysical model confirm this picture in general: for both data-sets, the best-fit thermal inertia is around 50 J m^{-2} s$^{-0.5}$ K^{-1}, about the thermal inertia of lunar regolith and somewhat higher than the typical thermal inertia of large main-belt asteroids (Müller et al. 1998). We caution, however, that our data-set is too small to conclusively determine Lutetia's thermal inertia; a thermal inertia of zero is compatible with our data.

Furthermore, our data indicate the possibility that the surface roughness might vary across the surface, with a preference for low roughness on the "southern" hemisphere (which was visible in 2004, when our IRTF observations took place) and high roughness around the equator (visible in 1983, when the IRAS measurements took place). We caution, however, that our data are inconclusive regarding surface roughness and further observations and modeling would be required to provide robust evidence of roughness variegation on Lutetia.

There will not be many opportunities for further observations of Lutetia before the planned Rosetta fly-by in 2010; the next one will be Lutetia's upcoming apparition in late 2005 and early 2006.

5. Conclusions

From new thermal-infrared spectrophotometric measurements and detailed thermophysical modeling we infer that Lutetia has a diameter of 98.3 ± 5.9 km and a geometric albedo of 0.208 ± 0.025, in good agreement with the results from IRAS radiometry (Tedesco 1992) and radar observations (Magri et al. 1999). We can rule out a low albedo typical of a C-type taxonomic classification as indicated by recent spectroscopic findings. Further spectroscopic observations should be made to check for variegation of spectral features with rotational phase and sub-Earth latitude.

Furthermore we confirm that Lutetia's surface must be covered with thermally-insulating material or regolith. A lunar-like thermal inertia of $\leq$100 J m^{-2} s$^{-0.5}$ K^{-1} is compatible with both our MIRSI data and the IRAS flux values.

Acknowledgements. The authors are visiting astronomers at the Infrared Telescope Facility, which is operated by the University of Hawaii under Cooperative Agreement no. NCC 5-538 with the National Aeronautics and Space Administration, Office of Space Science, Planetary Astronomy Program. We wish to thank Mikko Kaasalainen for making available the shape model of Lutetia. M. Mueller was supported in part by *Deutsche Forschungsgemeinschaft, DFG*.

References

Barucci, M. A., Fulchignoni, M., Fornasier, S., et al. 2005, A&A, 430, 313
Beichman, C. A., Neugebauer, G., Habing, H. J., et al. 1988, Infrared Astronomical Satellite (IRAS) Catalogs and Atlases, 1, Explanatory Supplement, NASA RP-1190
Birlan, M., Barucci, M. A., Vernazza, P., et al. 2004, New A, 9, 343
Bowell, E., Hapke, B., Domingue, D., et al. 1989, Application of photometric models to asteroids, in Asteroids II, ed. R. P. Binzel, et al., Univ. Arizon, Tucson, 524
Bus, S. J., & Binzel, R. P. 2002, Icarus, 158, 146
Cohen, M., Witteborn, F. C., Carbon, D. F., et al. 1996, AJ, 112, 2274
Cohen, M., Walker, R. G., Carter, B., et al. 1999, AJ, 117, 1864
Deutsch, L. K., Hora, J. L., Adams, J. D., et al. 2003, in Astronomical Telescopes and Instrumentation, Proc. SPIE, 4841, 106
Dotto, E., Müller, T. G., Barucci, M. A., et al. 2000, A&A, 358, 1133
Fowler, J. W., & Chillemi, J. R. 1992, IRAS data processing, in The IRAS Minor Planet Survey, ed. E. Tedesco, Tech. Rpt. PL-TR-92-2049, Phillips Laboratory, Hanscom Air Force Base, Massachusetts
Harris, A. W. 1998, Icarus, 131, 291
Harris, A. W., Mueller, M., Delbó, M., et al. 2005, Icarus, 179, 95
Howell, E. S., Merenyi, E., & Lebofsky, L. A. 1994, J. Geophys. Res., 99, 10847
Lagerros, J. S. V. 1996, A&A, 310, 1011
Lagerros, J. S. V. 1998, A&A, 232, 1123
Landolt, A. U. 1973, AJ, 78, 959
Lazzarin, M., Marchi, S., Magrin, S., et al. 2004, A&A, 425, L25
Lebofsky, L. A., Sykes, M. V., Tedesco, E. F., et al. 1986, Icarus, 68, 239
Lupishko, D. F., & Mohamed, R. A. 1996, Icarus, 119, 209
Magri, C., Ostro, S. J., Rosema, K. D., et al. 1999, Icarus, 140, 379
Mueller, M., Delbó, M., di Martino, M., et al. 2005, ASP Conf. Ser., submitted
Müller, T. G., & Lagerros, J. S. V. 1998, A&A, 338, 340
Müller, T. G., & Lagerros, J. S. V. 2002, A&A, 381, 324
Müller, T. G., Sterzik, M. F., Schütz, O., et al. 2004, A&A, 424, 1075
Rivkin, A. S., Howell, E. S., Lebofsky, L. A., et al. 2000, Icarus, 145, 351
Tedesco, E. F. 1992, The IRAS Minor Planet Survey. Tech. Rpt. PL-TR-92-2049, Phillips Laboratory, Hanscom Air Force Base, Massachusetts
Tholen, D. J. 1989, in Asteroids II, ed. R. P. Binzel, et al., Univ. Arizon, Tucson, 1139
Torppa, J., Kaasalainen, M., Michałowski, T., et al. 2003, Icarus, 164, 346
Walker, R. G. 2003, BAAS, 35, 980